Photocurrents Generated by Bacteriorhodopsin Adsorbed on Nano-Black Lipid Membranes

Christian Horn and Claudia Steinem
Institut für Analytische Chemie, Chemo- und Biosensorik, Universität Regensburg, Regensburg, Germany

ABSTRACT   Purple membranes were adsorbed on freestanding lipid bilayers, termed nano-black lipid membranes (nano-BLMs), suspending the pores of porous alumina substrates with average pore diameters of 280 nm. Nano-BLMs were obtained by first coating the upper surface of the highly ordered porous alumina substrates with a thin gold layer followed by chemisorption of 1,2-dipalmitoyl-*sn*-glycero-3-phosphothioethanol and subsequent addition of a droplet of 1,2-diphytanoyl-*sn*-glycero-3-phosphocholine and octadecylamine dissolved in *n*-decane onto the hydrophobic submonolayer. By means of impedance spectroscopy, the quality of the nano-BLMs was verified. The electrical parameters confirm the formation of single lipid bilayers with high membrane resistances covering the porous matrix. Adsorption of purple membranes on the nano-BLMs was followed by recording the photocurrents generated by bacteriorhodopsin upon continuous light illumination. The membrane system exhibits a very high long-term stability with the advantage that not only transient but also stationary currents are recordable. By adding the proton ionophore carbonyl cyanide-*m*-chlorophenylhydrazone the conductivity of the nano-BLMs increases, resulting in a higher stationary current, which proves that proton conductance occurs across the nano-BLMs.

INTRODUCTION

Bacteriorhodopsin (bR) is an integral membrane protein that uses light to translocate protons across membranes. It is found in highly ordered two-dimensional hexagonal arrays as purple patches in *Halobacterium salinarium*, termed purple membrane (1). bR is one of the most promising biomaterials that can be used for energy conversion, optoelectronics, optical storage information processing, and nonlinear optics. Its utility is based on its unique properties, such as extraordinary stability against thermal and photochemical degradation (2), fast photochemical reaction time, and the ability to sustain its biological activity when immobilized on solid supports (3).

Starting in the mid-1970s, adsorption of purple membranes on black lipid membranes (BLMs) has been used to study the light-induced charge translocation in a time-resolved manner (4–9). Low specific conductance and high specific capacitance of the BLMs lead to transient capacitive currents after activation of the ion pump; these currents provide information about the charge transport during the photocycle. The main advantage of using BLMs is their low conductance, which is the prerequisite for low noise measurements, and their high specific capacitance, yielding a large current signal. The major drawback, however, is their low mechanical and long-term stability preventing their usage in devices. To overcome this problem, Bamberg and coworkers first established lipid membranes immobilized on solid supports, to which purple membranes were attached (10). Using this device, charge transport of the light-activated

proton pump can still be studied in an environment similar to that provided by BLMs but with a much larger stability. However, owing to the direct coupling of the membrane to the polarizable gold electrode, the underlying capacitance prevents the establishment of a stationary current, i.e., proton conductance is prevented.

Recently, we have described a new model membrane system that combines the properties of solid-supported and black lipid membranes, which we termed nano- and micro-BLMs, respectively (11,12). For nano-BLMs, a highly ordered, porous alumina substrate with a pore size of 280 nm serves as a ''solid support''. The porous material can be easily produced, making it well suited for its application in biosensor devices (13–15). Nano-BLMs were prepared from a lipid solution in *n*-decane after functionalizing the upper surface of the porous material with 1,2-dipalmitoyl-*sn*-glycero-3-phosphothioethanol (DPPTE), rendering it hydrophobic. On one side (the *cis* side) of the nano-BLMs, purple membranes were attached, resulting in an extraordinarily high long-term stable membrane system that allows the sensitive detection of light-induced proton currents of bR. Due to the aqueous compartment on the opposite side (the *trans* side) provided by the porous alumina, not only can transient photocurrents be observed, as in the case of solid-supported membranes (SSMs), but also stationary currents can be established, which cannot be achieved by SSMs.

MATERIALS AND METHODS

Materials

Aluminum substrates (thickness 0.5 mm, purity 99.999%) were purchased from Goodfellow (Huntingdon, UK). DPPTE and 1,2-diphytanoyl-*sn*-glycero-3-phosphocholine (DPhPC) were obtained from Avanti Polar Lipids (Alabaster, AL). Purple membranes were isolated according to

standard procedures from *Halobacterium salinarium* (16). Carbonyl cyanide *m*-chlorophenylhydrazone (CCCP) was purchased from Sigma-Aldrich (Munich, Germany). The water used was ion-exchanged and millipore-filtered (Milli-Q-System, Millipore, Molsheim, France; specific resistance $R > 18$ MΩ cm^{-1}, pH 5.5).

Preparation and functionalization of porous alumina substrates

The preparation of highly ordered porous alumina substrates has been described previously (11). Briefly, cleaned and electropolished aluminum foils were anodized in aqueous phosphoric acid solution (5 wt %) at $T = 2°C$ and $V = 160$ V for 48 h. The resulting porous alumina substrate was then treated with a saturated HgCl$_2$-solution to remove the underlying aluminum layer. Finally, the alumina pore bottoms were removed by chemical etching at 30°C in 5 wt % phosphoric acid solution. The resulting sievelike structure has a mean thickness of ~200 μm as determined by scanning electron microscopy images of cross sections. The bottom surface of the porous substrate was coated with a thin gold layer (40–70 nm) using a sputter coater with a thickness control unit (Cressington sputter coater 108auto, Cressington MTM-20, Elektronen-Optik-Service, Dortmund, Germany). The gold coating allowed for the chemisorption of DPPTE from a 0.5-mM ethanolic solution ($t > 12$ h), rendering the surface hydrophobic. After thoroughly rinsing with ethanol and drying under a stream of nitrogen, the porous sample was mounted in the teflon cell (Fig. 1).

Formation of nano-BLMs and adsorption of purple membranes

After the substrate was vertically placed in the Teflon cell (Fig. 1), the *cis* and *trans* compartments were filled with electrolyte solution composed of 10 mM Tris-HCl, 0.1 M KCl, pH 7.4. A solution of 1,2-diphytanoyl-*sn*-glycero-3-phosphocholine (DPhPC) (1% w/v) and octadecylamine (ODA) (0.025% w/v) dissolved in *n*-decane was painted across the DPPTE-functionalized surface oriented to the *cis* side. After impedance analysis of the formed nano-BLM, purple membranes that had been sonicated for ~2 min were added to the *cis* compartment while stirring the solution, leading to a final bacteriorhodopsin concentration of 0.01 mg/ml.

Impedance spectroscopy

Porous alumina substrates and lipid membrane-covered porous alumina were investigated using impedance spectroscopy. The impedance gain/phase analyzer SI 1260 and the 1296 Dielectric Interface (Solartron Instruments,
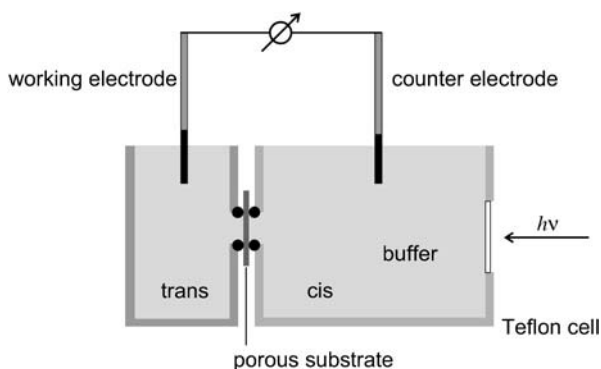

FIGURE 1 Experimental setup. Two Teflon half-cells with the porous alumina substrate clamped in between were used for impedance analysis and photocurrent measurements. Electrical contact was achieved by platinized platinum electrodes in both cuvettes.

Farnborough, UK), controlled by a personal computer were used for AC impedance analysis. The absolute value of the impedance $|Z|(f)$ and the phase angle $\phi(f)$ between voltage and current were recorded within a frequency range of 10^{-2}–10^6 Hz, with equally spaced data points on a logarithmic scale and with five data points per decade, which took ~12 min. All data were obtained at zero offset potential applying a small AC voltage of 30 mV to avoid nonlinear responses. Data recording was performed using the Solartron Impedance Measurement Software (version 3.5.0), and data analysis using the software package Zview2.6b with Calc-Modulus data weighting. The Teflon cell used for mounting the porous substrate was the same for impedance and photocurrent measurements and is described in the next section.

Photocurrent measurements

Two Teflon half-cells were separated by the porous alumina substrate with a total area of 7 mm^2 sealed by an O-ring (Fig. 1). Platinized platinum wires, immersed in the electrolyte solution on both sides, serve as working (*cis* compartment) and counter (*trans* compartment) electrodes. For photocurrent measurements, the electrodes were separated from the measuring cell by salt bridges to minimize photoartifacts. Illumination of the membrane-covered porous surface with a 250-W halogen lamp (KL2500, Opto Sonderbedarf, Gräfelfing, Germany) was achieved through a glass window in the *cis* compartment. The relative light intensity was adjusted by a dimming function of the lamp. The light was filtered with a 515-nm cut-off filter and guided into a darkened Faraday cage by an optical fiber. A mechanical shutter operated by a wire release was used for switching the light on and off. The current generated by illuminating the purple membranes adsorbed on the nano-BLMs was measured with a current amplifier (Keithley 428, Keithley Instruments, Germering, Germany) and data was transferred via a GPIB interface to a personal computer using an acquisition program written in Labview 6.0. For obtaining an action spectrum presented as the initial current density as a function of wavelength, narrow-band interference filters (AHF Analysentechnik, Tübingen, Germany, half-width 10 nm) were used.

RESULTS

Impedance analysis of nano-BLM formation

Each nano-BLM formation was monitored by means of impedance spectroscopy. This method enables us to follow the formation process and to determine the electrical properties of each nano-BLM as a measure of its quality. The procedure is described in more detail elsewhere (11). Briefly, impedance spectra were taken in a frequency range of 10^{-2}–10^6 Hz, and electrical parameters of the system were extracted by using an equivalent circuit composed of a parallel connection of a resistance R_m and capacitance C_m, representing the electrical properties of the nano-BLM serial to the Ohmic resistance R_{el} representing the electrolyte solution. If the resistance was <10 MΩ and could not be detected within the observed frequency range, R_m was ignored in the fitting routine. A nano-BLM preparation was called successful if the capacitance was $C_m = (0.5 \pm 0.3)$ μF/cm^2 while the membrane resistance R_m was > 0.1 GΩ. After the formation of a nano-BLM, purple membranes (PM) were added to the *cis* compartment. A typical impedance spectrum is shown in Fig. 2. The adsorption of the PM fragments, which was followed by recording the corresponding photocurrents (see below), did not alter the electrical parameters of the system.
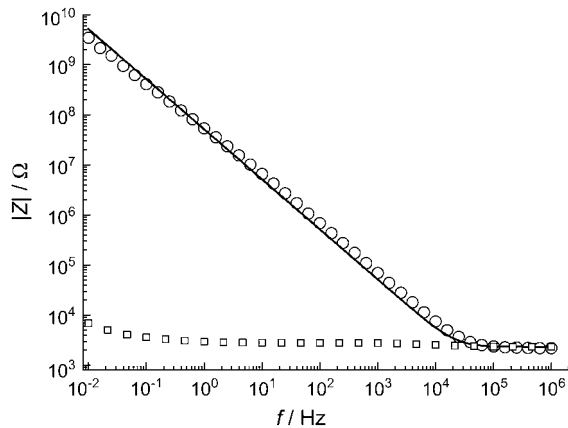
FIGURE 2   Impedance spectra of a gold-covered porous alumina substrate functionalized with a DPPTE submonolayer before (□) and after (○) spreading of a lipid droplet across the porous substrate. The solid line is the result of the fitting procedure using an equivalent circuit composed of a serial connection the electrolyte resistance R_{el} and the capacitance C_m of the lipid bilayer, which was determined to be $C_m = 0.77$ $\mu F/cm^2$.

Adsorption of purple membranes

To attach purple membranes to the nano-BLMs, a PM suspension was added to the cuvette while stirring the solution. The adsorption process of PM fragments was followed by monitoring the photocurrents developing over time. A typical current trace is depicted in Fig. 3 A. The direction of the positive current corresponds to the translocation of protons from the *cis* to the *trans* compartment when switching the light on. The current signal is characterized by two transient currents, one upon switching the light on and the other upon switching it off. For the calculation of the current density the measured current was divided by the "active area" of 2.3 mm^2, which corresponds to the product of the geometric sample area and the porosity of the sample (11). First, the current density rises to a maximum value J_{max-on}, which is 170 nA/cm^2, and then decays with a characteristic decay time τ_{on} to the stationary current density of $J_{stat} = 3$ nA/cm^2, indicating that even without a proton ionophore there is a small proton conductivity of the nano-BLM. Upon switching the light off, a second transient current density $J_{max-off}$ is observed which decays to zero. To ensure that the observed current traces are not a result of a photoartifact, nano-BLMs were illuminated before the addition of PM fragments (Fig. 3 A). No such transient currents were observed.

The maximum peak current density J_{max-on} was chosen to monitor the adsorption process of the PM fragments from the stirred solution by recording the time-dependent evolution of the photocurrents (Fig. 3 B). Already 10 min after the addition of purple membranes to the *cis* compartment, light-induced currents were monitored. The maximum current density further increases over time, indicating the continuous adsorption of purple membranes on the nano-BLM until J_{max-on} reaches a value of 160 nA/cm^2 after 40 min. This fast
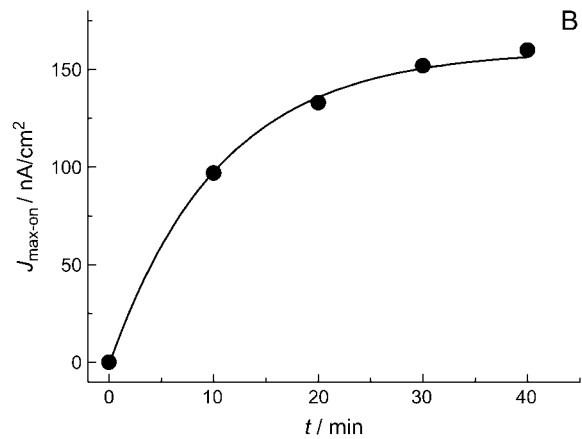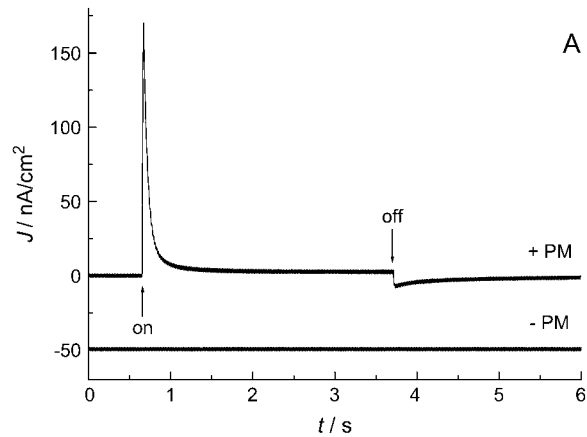

FIGURE 3   (A) Photocurrent before (− PM) and after (+ PM) addition of purple membranes to the *cis* compartment. (+ PM) The first transient corresponds to switching the light on, the second transient to switching the light off. The current was recorded 40 min after addition of purple membranes. (− PM) The current trace corresponds to the signal recorded before addition of purple membranes. No significant photoartifact can be detected. For clarity, the current trace is shifted by −50 nA/cm^2. (B) Time course of the maximum current density J_{max-on} after addition of purple membranes. J_{max-on} saturates after ~40 min. The solid line is the result of a monoexponential fit to the data and serves as a guide for the eye.

adsorption process, leading to an almost constant maximum current density J_{max-on} after 40 min, is followed by a very slow process resulting in a continuous but very slow increase in J_{max-on}. After 3 days, J_{max-on} has reached a value of ~300 nA/cm^2 (see Fig. 7 B). This observation might be explained by further adsorption of PM fragments and their possible lateral reorganization. In general, the maximum current densities always showed the same overall time-dependent behavior but differed in their absolute magnitudes, indicating that the amount and orientation of the purple membranes adsorbed on the nano-BLMs is different. Exchanging the purple membrane-containing solution for pure buffer did not alter the shape and magnitude of the observed photocurrents, demonstrating that once the PM fragments have been adsorbed on the nano-BLM they are irreversibly bound.

Action spectrum

To show that the light-induced signal after the addition of purple membranes reflects the electrical activity of bacteriorhodopsin, narrow band filters were used to obtain an action spectrum of the current signals. Fig. 4 (*solid circles*) shows the action spectrum represented as the normalized peak current density. The dashed line is a Gaussian function fitted to the spectrum. A peak maximum of $\lambda_{max} = 548$ nm is obtained. For comparison, the absorption spectrum of purple membranes in solution was taken and plotted as a solid line. The characteristic maximum absorbance of bacteriorhodopsin at 568 nm was found. Apparently, adsorption of the purple membranes on nano-BLMs leads to an action spectrum that is shifted by $\sim$20 nm compared to the absorption spectrum in solution.

Light intensity

According to theory (see Supplementary Material), the maximum current densities after switching the light on and off are supposed to be light-dependent (see Eqs. 2a, 5a, and 3 in Supplementary Material). Fig. 5 A shows J_{max} obtained for switching the light on (J_{max-on}) and off ($J_{max-off}$), as a function of light intensity. With increasing light intensity the maximum current density increases for switching the light on. The maximum current density for switching the light off is negative, however, and becomes more negative for larger light intensities. Both current densities saturate with increasing light intensity, consistent with theory (see Supplementary Material). Fig. 5 B shows the reciprocal relaxation time τ as a function of light intensity for the light-on (τ_{on}) and light-off (τ_{off}) processes. According to theory, only τ_{on} is light-dependent, whereas τ_{off} is light-independent, consistent with the obtained data (see Eqs. 2c and 5b, Supplementary Material).

FIGURE 5 (*A*) Maximum current density J_{max} as a function of light intensity: (●), J_{max-on}; (■), $J_{max-off}$. (*B*) Reciprocal decay time constant τ of the photocurrent as a function of light intensity: (●), τ_{on}, (■), τ_{off}. The solid lines are the results of fitting the parameters of Eqs. 2a (J_{max-on}), 2c (τ_{on}), and 5a ($J_{max-off}$) (see Supplementary Material) to the data with the following parameters: $C_m = 1$ μF/cm^2 (fixed); $C_p = 2$ μF/cm^2 (fixed); $G_m = 10$ nS/cm^2 (fixed); $G_p = 1$ μS/cm^2 (fixed); $J_{p0}^s = (930 \pm 30)$ nA/cm^2; $L_{1/2} = (0.5 \pm 0.1)$; and $V^* = (0.010 \pm 0.001)$ V. τ_{off} is independent of the light intensity.

Influence of CCCP

In contrast to solid-supported membranes on gold surfaces, nano-BLMs allow measuring stationary currents of bacteriorhodopsin dependent on the proton conductance of the underlying lipid bilayer due to the presence of a second compartment. To increase the proton conductance, the membrane-soluble proton ionophore CCCP was added to the *cis* compartment. CCCP facilitates the diffusion of protons pumped from bacteriorhodopsin toward the nano-BLM into the pores of the underlying alumina substrate. The impact of the addition of CCCP on the light-induced ionic current is shown in Fig. 6 A. After switching the light on, a transient current is again first observed followed by a significant stationary current of $\sim$47 nA/cm^2 for a 10-μM CCCP concentration in solution and 72 nA/cm^2 for 40 μM. To investigate whether the stationary current changes over time, the membrane was illuminated for 10 min. The
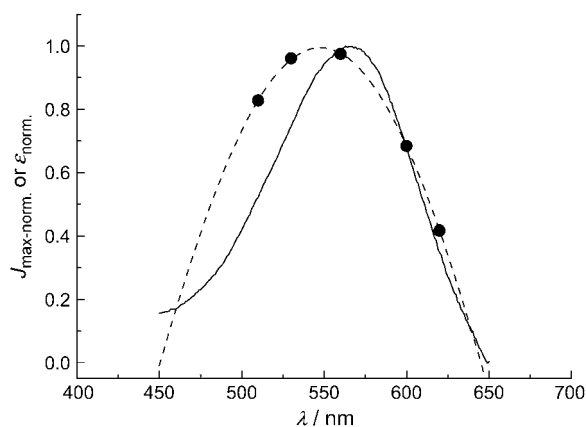

FIGURE 4 (●) Action spectrum of bacteriorhodopsin in purple membranes adsorbed on nano-BLMs presented as the normalized maximum initial current density ($J_{max}/J_{max(max)}$) measured with a series of narrow-band interference filters. The maximum current densities were corrected by the lamp spectrum. A Gaussian function was fitted to the data, shown as a dashed line. The solid line shows the normalized absorption spectrum ($\varepsilon/\varepsilon_{(max)}$) of a purple membrane suspension.
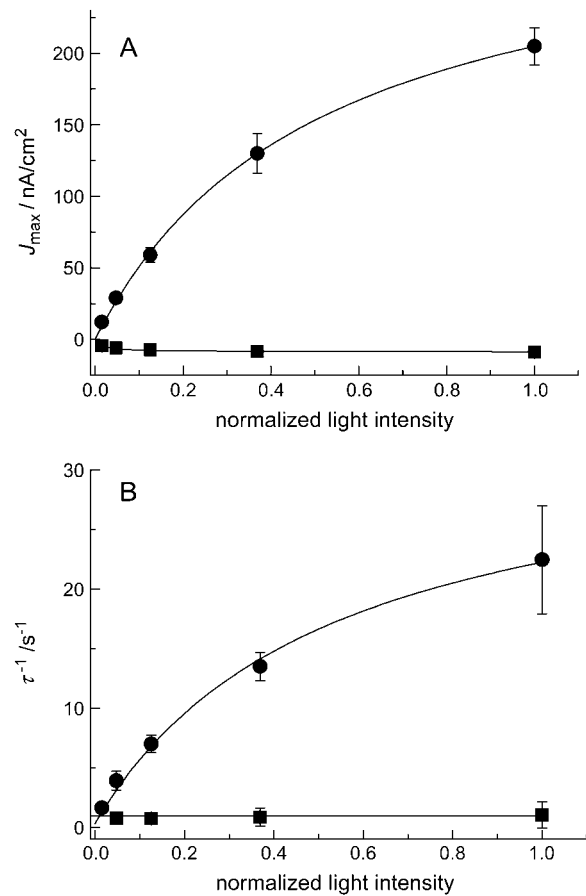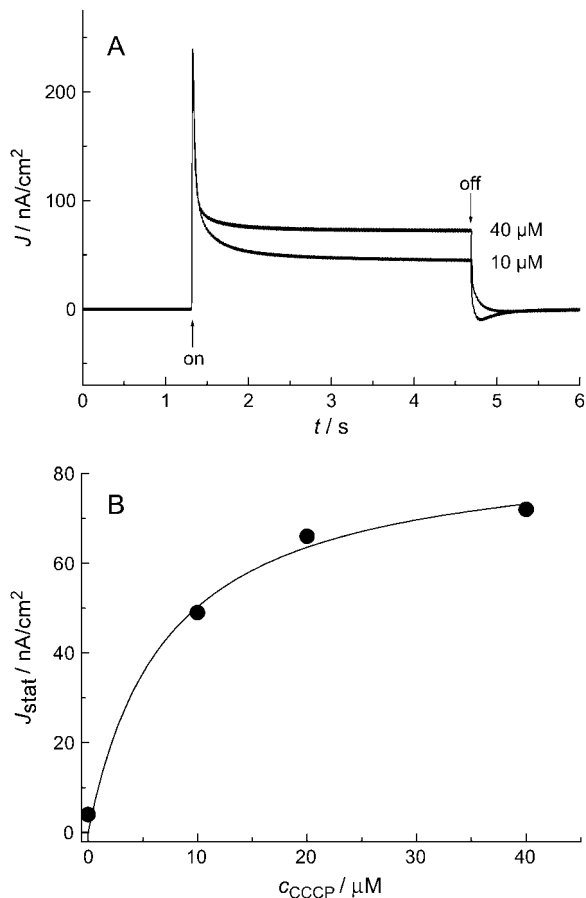
FIGURE 6 (*A*) Photocurrent 15 min after the addition of 10 and 40 μM CCCP. (*B*) Stationary current density J_{stat}, obtained 1.5 s after switching the light on as a function of the CCCP concentration in solution. The solid line demonstrates the saturation behavior as expected from Eq. 4 (see Supplementary Material).

for possible devices based on bR technology. To monitor the long-term stability, the change in membrane resistance R_m, maximum current density J_{max-on}, and stationary current density J_{stat} were chosen as characteristic parameters. Fig. 7 shows the time change of the three parameters monitored after preparation of a nano-BLM, followed by the adsorption of purple membranes and the addition of the proton ionophore CCCP with a concentration of 40 μM. After 3 days the *cis* compartment was carefully rinsed with buffer to remove PM fragments from solution. Fig. 7 *A* shows the membrane resistance R_m versus time. Starting with a value of 0.1 GΩ, the resistance decreases within 18 days to a value of 0.46 MΩ. Rinsing with buffer after 3 days did not significantly alter the membrane resistance, indicating that the membrane is still intact. The continuous decrease of R_m is interpreted as decoupled membrane areas that rupture independently of each other so that the membrane resistance decreases gradually rather than in a one-step process as with classical BLMs. Besides R_m, the maximum current density J_{max-on} and the stationary current density J_{stat} were monitored

stationary current remained constant within this time period. The influence of the CCCP concentration in solution on the stationary current was investigated in more detail, and it was demonstrated that it increases with increasing CCCP concentration and saturates at a concentration of ~40 μM (Fig. 6 *B*).

Long-term stability

The experiments described above demonstrate that in principle the photocurrents obtained from purple membranes adsorbed on nano-BLMs are similar to those obtained using classical BLMs as the substrate (6). Even stationary currents can be monitored as a function of the proton conductance of the underlying nano-BLM, which cannot be achieved by using solid-supported membranes. However, classical BLMs lack mechanical and long-term stability, preventing the development of bR-based devices. Nano-BLMs exhibit a much higher long-term stability (11), which is in the order of several tens of hours, and are thus promising candidates

FIGURE 7 (*A*) Time dependence of the membrane resistance R_m of a nano-BLM with adsorbed purple membrane fragments. R_m was extracted from the corresponding impedance spectra. The horizontal dashed line shows the electrolyte resistance R_{el}, demonstrating the value that is reached after completely rupturing the nano-BLM. (*B*) Time dependence of the maximum current density (■) and the stationary current density (▲) on a large timescale.

over time (Fig. 7 *B*). Within the observed time period, $J_{max\text{-}on}$ remained constant at (310 ± 10) nA/cm^2. After three days, a slight change of $J_{max\text{-}on}$ was observed after rinsing with buffer, which is, however, within the error of the experiment. The result suggests that purple membranes stick irreversibly on the nano-BLMs without losing activity. Starting with a value of 73 nA/cm^2, the stationary current density J_{stat} drops slightly after rinsing with buffer after 3 days, but then stays constant with a value of (41 ± 7) nA/cm^2.

In Fig. 7, the results of an extraordinary stable membrane preparation of purple membranes adsorbed on nano-BLMs are displayed. After 18 days the porous alumina substrate was rinsed with ethanol and buffer solution to rupture the nano-BLM. After this procedure, a membrane resistance could not be monitored any longer by impedance spectroscopy; only the electrolyte resistance was discernable (see Fig. 7 *A*, *dotted line*). Likewise, no photocurrent was measured anymore upon illumination, confirming that indeed the observed photocurrents were a result of active bacteriorhodopsin immobilized on nano-BLMs. In most cases, preparations of nano-BLMs with adsorbed purple membranes were less stable but always lasted several days.

DISCUSSION

Throughout literature, purple membranes have been adsorbed on many substrates to investigate the light-induced photocurrent generated by bacteriorhodopsin. Substrates include membranes such as BLMs (4–9) and SSMs (10,17,18), tin oxide (19–21), gold surfaces (22–24), and polycation layers (21,25,26). Possible applications for such systems have been proposed in emerging areas like biosensors, bioelectronics, biooptics, and biocomputing (27–30). Especially BLMs and SSMs are well-suited for the investigation of electrical properties of ion-translocating proteins like bacteriorhodopsin. However, BLMs suffer from short lifetimes. This problem can be overcome by using SSMs that exhibit a high long-term stability but do not allow measuring stationary currents due to the capacitance of the underlying support serving as the electrode. Recently, we reported on membrane systems that we call nano-BLMs and micro-BLMs, which overcome the drawbacks of the above-mentioned model systems (11,12). Here, we applied these nano-BLMs to attach purple membrane fragments to obtain a long-term stable membrane system that additionally allows the monitoring of stationary currents generated by immobilized bR (Fig. 8 *A*).

By means of impedance spectroscopy the insulating properties of those membranes were investigated. The resistance R_m and capacitance C_m of the nano-BLMs were extracted by applying an appropriate equivalent circuit to the spectra. Impedance analysis revealed that the membrane resistance is in the GΩ regime, which is required for low noise-current measurements. Low conductance is essential as the nano-BLMs are only partly covered by adsorbed purple membranes. Without an underlying high resistive nano-BLM the
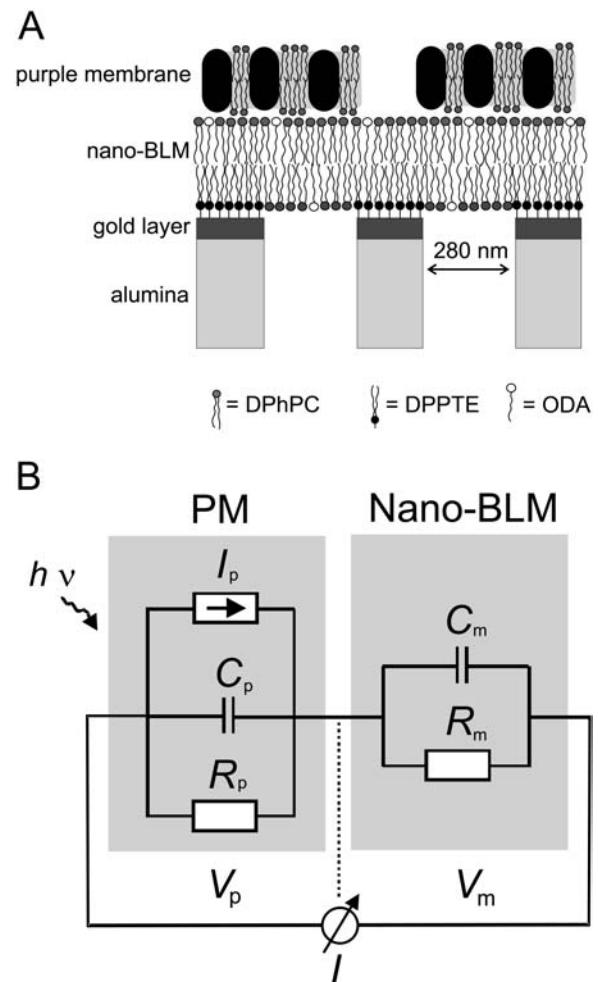

FIGURE 8 (*A*) Schematic representation of adsorbed purple membranes on nano-BLMs. (*B*) Electrical equivalent circuit representing light-activated bacteriorhodopsin adsorbed on nano-BLMs. C_m and R_m represent the capacitance and resistance of the nano-BLM, whereas C_p and R_p are the capacitance and resistance, respectively, of the purple membrane. I_p is the light-driven proton current generated by bacteriorhodopsin. Under short-circuit conditions, the voltage drop across the membrane V_m equals that across the purple membranes V_p. I is the measured current.

noncovered area would act as a shunt resistance generating a high background noise level. To obtain specific capacitances, the estimated porous area obtained from scanning electron microscope images was taken into account, as the ionic current flows only through the pores of the alumina substrate. The calculated mean specific capacitance of (0.5 ± 0.3) μF/cm^2 for the nano-BLMs is in the same range as those obtained for classical BLMs, which are reported to be ~ 0.5 μF/cm^2 (31,32), and for membranes suspending an aperture of a micromachined support, which are reported to be in the range of 0.3–1.1 μF/cm^2 (33–36). The capacitances thus demonstrate the formation of single lipid bilayers. After adsorption of purple membranes on preformed nano-BLMs the capacitance of the system does not change, supporting

the theory that purple membranes do not form a closely packed layer.

Once a stable nano-BLM was formed, purple membranes were adsorbed onto it, which was followed by measuring the light-induced current as a function of time. From the time course of the maximum transient current density $J_{\text{max-on}}$, which saturates after ~40 min (see Fig. 3), one might safely assume that the majority of purple membrane binding sites are occupied. The overall time course of $J_{\text{max-on}}$ suggests, however, that adsorption is accompanied by lateral re-organization of the membrane patches on a much slower timescale, eventually resulting in a larger coverage due to higher packing of the patches than is achieved by pure irreversible adsorption. Photoartifacts, seen in the illumination of solid supported membranes immobilized on gold electrodes (10,37), were not observed using nano-BLMs on porous alumina.

To further prove that the proton currents are a result of bacteriorhodopsin activity, an action spectrum was measured by monitoring the initial current density using a series of narrow-band filters. Compared to the absorption spectrum of purple membranes in solution, the action spectrum obtained from purple membranes adsorbed on nano-BLMs is shifted by ~20 nm, from 568 to 548 nm. This observation is in accordance with previously published results, where purple membranes were attached to classical black lipid membranes (6). An action spectrum of the stationary current was monitored that was blue-shifted by ~15 nm compared to the absorption spectrum of purple membranes in solution.

The observed photocurrents induced by the light-activated proton pump bacteriorhodopsin are characterized by a positive net current of protons from the *cis* to the *trans* compartment, when switching the light on. Since the adsorption of purple membranes is partially driven by the electrostatic interaction between the negatively charged membrane fragments and the positively charged detergent octadecylamine in the nano-BLM, the favored orientation might be influenced by the surface charge density of the cytoplasmic surface, which is determined to be $-0.22\ \text{C/m}^2$, and of the extracellular surface, which is calculated to be only $-0.08\ \text{C/m}^2$ at neutral pH (38,39). This difference in surface charge density would imply a preferential attachment of the cytoplasmic surface to the bilayer, whereas the extracellular side faces the *cis* compartment, which would in principle result in a proton transport direction from the nano-BLM toward the solution (the *cis* compartment). Since the proton transport is observed in the opposite direction, at least part of the purple membrane fragments are oriented in the other direction and the current is dominated by this purple membrane fraction. It is also well conceivable that not the surface charge density but the different morphologies of the extracellular and cytoplasmic sides of the PM leads to a preferential adsorption with the extracellular side facing the nano-BLM.

Our system enables us to measure not only transient but also stationary currents. Stationary currents as a function of

proton permeability were also observed by others. Upon addition of gramicidin A to a classical BLM decorated with adsorbed purple membranes, Bamberg et al. (6) also observed a stationary current from the *cis* to the *trans* compartment. In our case, the protons must flow from the purple membrane across the nano-BLM facilitated by the proton ionophore CCCP into the pores of the underlying porous alumina substrate. Since the stationary current does not decrease within a time period of 10 min of continuous illumination, we conclude that the pores do not form an observable diffusion barrier for protons. Hence, the theoretical considerations developed for black lipid membranes can be adapted (6), leading to the equivalent circuit depicted in Fig. 8 *B*, which models the system of purple membranes adsorbed on nano-BLMs. C_{p} and R_{p} are the capacitance and resistance, respectively, of the purple membrane, whereas I_{p} is the light-driven current generated by bR. The underlying nano-BLM is characterized by the capacitance C_{m} and the resistance R_{m}. According to this theoretical approach, the stationary current I_{stat} depends on the conductance $G_{\text{m}} = R_{\text{m}}^{-1}$ of the nano-BLM (Eq. 2b). As G_{m} is proportional to the aqueous CCCP concentration (40), I_{stat} is expected to also depend on the CCCP-concentration according to Eq. 4, as demonstrated in Fig. 6.

Our results demonstrate that, in principle, we are able to obtain results similar to those for classical BLMs with adsorbed purple membranes. In contrast to classical BLMs, nano-BLMs exhibit a much larger mechanical and long-term stability. In a previous publication, we reported on nano-BLM preparations that were stable for several tens of hours and allowed for single ion-channel measurements for 1–2 days (11). Although for the measurement of bR-induced photocurrents a large membrane resistance is required, GΩ resistances, which are a prerequisite for monitoring single-channel events, are not essential. Thus, the stability in terms of constant maximum and stationary photocurrents is extraordinarily large. Even though the membrane resistance slowly decreases over time within a period of days, the maximum current density and the stationary current density remain constant for at least several days. In one experiment, we obtained a membrane preparation that was stable for 18 days. After 18 days the membrane was destroyed. This very high long-term stability, even compared to nano-BLMs without adsorbed purple membranes, might be explained as follows: Regions of the membrane that are not covered by purple membranes partially rupture and thus cause the slow decrease of the membrane resistance. In contrast, nano-BLMs that are covered by purple membranes are stabilized by the rigid membrane sheets. A purple membrane patch is typically 1–5 μm in diameter (41) and thus covers ~7–170 membrane-suspended pores. Desorption of the purple membrane does not occur as long as the membrane is stable. Thus, the photocurrents are constant on a large timescale even though the membrane resistance of the nano-BLM slowly decreases.

CONCLUSIONS

Nano-BLMs are a hybrid system combining the merits of classical BLMs and solid supported membranes, and appear to be well suited for the development of membrane-based biosensors. The enormous increase in long-term and mechanical stability, together with the fact that the membranes are attached to a ''solid support'', make it possible to apply them in biosensor and chip technology and for the development of photoresponsive intelligent materials.

SUPPLEMENTARY MATERIAL

An online supplement to this article can be found by visiting BJ Online at http://www.biophysj.org.

REFERENCES

1. Oesterhelt, D., and W. Stoeckenius. 1973. Functions of a new photoreceptor membrane. *Proc. Natl. Acad. Sci. USA*. 70:2853–2857.

2. Shen, Y., C. R. Safinya, K. S. Liang, A. F. Ruppert, and K. J. Rothschild. 1993. Stabilization of the membrane protein bacteriorhodopsin to 140°C in two-dimensional films. *Nature*. 366:48–50.

3. Miyasaka, T., K. Koyama, and K. Itoh. 1992. Quantum conversion and image detection by a bacteriorhodopsin-based artificial photoreceptor. *Science*. 255:342–344.

4. Drachev, L. A., A. A. Jasaitis, A. D. Kaulen, A. A. Kondrashin, E. A. Liberman, I. B. Nemecek, S. A. Ostroumov, A. Y. Semenov, and V. P. Skulachev. 1974. Direct measurement of electric current generation by cytochrome oxidase, H^+-ATPase and bacteriorhodopsin. *Nature*. 249:321–324.

5. Danzshazy, Z., and B. Karvaly. 1976. Incorporation of bacteriorhodopsin into a bilayer lipid membrane: a photoelectric-spectroscopic study. *FEBS Lett.* 72:136–138.

6. Bamberg, E., H.-J. Apell, N. A. Dencher, W. Sperling, H. Stieve, and P. Läuger. 1979. Photocurrents generated by bacteriorhodopsin on planar bilayer membranes. *Biophys. Struct. Mech.* 5:277–292.

7. Tittor, J., U. Schweiger, D. Oesterhelt, and E. Bamberg. 1994. Inversion of proton translocation in bacteriorhodopsin mutants D85N, D85T, and D85,96N. *Biophys. J.* 67:1682–1690.

8. Fahr, A., P. Läuger, and E. Bamberg. 1981. Photocurrent kinetics of purple-membrane sheets bound to planar bilayer membranes. *J. Membr. Biol.* 60:51–62.

9. Ganea, C., J. Tittor, E. Bamberg, and D. Oesterhelt. 1998. Chloride- and pH-dependent proton transport by BR mutant D85N. *Biochim. Biophys. Acta*. 1368:84–96.

10. Seifert, K., K. Fendler, and E. Bamberg. 1993. Charge transport by ion translocating membrane proteins on solid supported membranes. *Biophys. J.* 64:384–391.

11. Römer, W., and C. Steinem. 2004. Impedance analysis and single-channel recordings on nano-black lipid membranes based on porous alumina. *Biophys. J.* 86:955–965.

12. Römer, W., Y. H. Lam, D. Fischer, A. Watts, W. B. Fischer, P. Göring, R. B. Wehrspohn, U. Gösele, and C. Steinem. 2004. Channel activity of a viral transmembrane peptide in micro-BLMs: Vpu$_{1–32}$ from HIV-1. *J. Am. Chem. Soc.* 126:16267–16274.

13. Jessensky, O., F. Müller, and U. Gösele. 1998. Self-organized formation of hexagonal pore arrays in anodic alumina. *Appl. Phys. Lett.* 72:1173–1175.

14. Li, A. P., F. Müller, A. Birner, K. Nielsch, and U. Gösele. 1998. Hexagonal pore arrays with a 50–420 nm interpore distance formed by self-organization in anodic alumina. *J. Appl. Phys.* 84:6023–6026.

15. Li, A. P., F. Müller, A. Birner, K. Nielsch, and U. Gösele. 1999. Fabrication and microstructuring of hexagonally ordered two-dimensional nanopore arrays in anodic alumina. *Adv. Mater.* 11:483–487.

16. Oesterhelt, D., and W. Stoeckenius. 1974. Isolation of the cell membrane of *Halobacterium halobium* and its fractionation into red and purple membrane. *Methods Enzymol.* 31:667–678.

17. Dolfi, A., F. Tadini Buoninsegni, M. R. Moncelli, and R. Guidelli. 2002. DC photoelectric signals from bacteriorhodopsin adsorbed on lipid monolayers and thiol/lipid bilayers supported by mercury. *Bioelectrochemistry*. 56:151–156.

18. Dolfi, A., F. Tadini-Buoninsegni, M. R. Moncelli, and R. Guidelli. 2002. Photocurrents generated by bacteriorhodopsin adsorbed on thiol/lipid bilayers supported by mercury. *Langmuir*. 18:6345–6355.

19. Wang, J.-P., S.-K. Yoo, L. Song, and M. A. El-Sayed. 1997. Molecular mechanism of the differential photoelectric response of bacteriorhodopsin. *J. Phys. Chem. B.* 101:3420–3423.

20. Li, Q., J. A. Stuart, R. R. Birge, J. Xu, A. Stickrath, and P. Bhattacharya. 2004. Photoelectric response of polarization sensitive bacteriorhodopsin films. *Biosens. Bioelectron.* 19:869–874.

21. Chu, J., X. Li, J. Zhang, and J. Tang. 2003. Fabrication and photoelectric response of poly(allylamine hydrochloride)/PM thin films by layer-by-layer deposition technique. *Biochem. Biophys. Res. Commun.* 305:116–121.

22. Choi, H.-G., J. Min, W. H. Lee, and J.-W. Choi. 2002. Adsorption behavior and photoelectric response characteristics of bacteriorhodopsin thin films fabricated by self-assembly technique. *Colloids Surf. B.* 23:327–337.

23. Chen, D., Y. Lu, S. Sui, B. Xu, and K. Hu. 2003. Oriented assembly of purple membrane on solid support mediated by molecular recognition. *J. Phys. Chem. B.* 107:3598–3605.

24. Miyasaka, T., T. Atake, and T. Watanabe. 2003. Generation of photoinduced steady current by purple membrane Langmuir-Blodgett films at electrode-electrolyte interface. *Chem. Lett.* 32:144–145.

25. He, J.-A., L. Samuelson, L. Li, J. Kumar, and S. K. Tripathy. 1998. Oriented bacteriorhodopsin/polycation multilayers by electrostatic layer-by-layer assembly. *Langmuir*. 14:1674–1679.

26. Salditt, T., and U. S. Schubert. 2002. Layer-by-layer self-assembly of supramolecular and biomolecular films. *Rev. Mol. Biotechnol.* 90:55–70.

27. Nicolini, C., V. Erokhin, S. Paddeu, C. Paternolli, and M. K. Ram. 1999. Toward bacteriorhodopsin based photocells. *Biosens. Bioelectron.* 14:427–433.

28. Wise, K. J., N. B. Gillespie, J. A. Stuart, M. P. Krebs, and R. R. Birge. 2002. Optimization of bacteriorhodopsin for bioelectronic devices. *Trends Biotechnol.* 20:387–394.

29. Zhang, L., T. Zeng, K. Cooper, and R. O. Claus. 2003. High-performance photovoltaic behavior of oriented purple membrane polymer composite films. *Biophys. J.* 84:2502–2507.

30. Wise, K. J., and R. R. Birge. 2004. Biomolecular photonics based on bacteriorhodopsin. W. Horspool and F. Lenci, editors. CRC Press, Boca Raton, FL.

31. Benz, R., O. Fröhlich, P. Läuger, and M. Montal. 1975. Electrical capacity of black lipid films and of lipid bilayers made from monolayers. *Biochim. Biophys. Acta*. 394:323–334.

32. Tien, H. T., and A. L. Ottova. 2000. Membrane biophysics: planar lipid bilayers and spherical liposomes. Elsevier, Amsterdam.

33. Cheng, Y., R. J. Bushby, S. D. Evans, P. F. Knowles, R. E. Miles, and S. D. Ogier. 2001. Single ion channel sensitivity in suspended bilayers on micromachined supports. *Langmuir.* 17:1240–1242.

34. Pantoja, R., D. Sigg, R. Blunck, F. Bezanilla, and J. R. Heath. 2001. Bilayer reconstitution of voltage-dependent ion channels using a microfabricated silicon chip. *Biophys. J.* 81:2389–2394.

35. Fertig, N., C. Meyer, R. H. Blick, C. Trautmann, and J. C. Behrends. 2001. Microstructured glass chip for ion-channel electrophysiology. *Phys. Rev. E.* 64:1–4.

36. Peterman, M. C., J. M. Ziebarth, O. Braha, H. Bayley, H. A. Fishman, and D. M. Bloom. 2002. Ion channels and lipid bilayer membranes under high potential using microfabricated apertures. *Biomed. Microdevices.* 4:231–236.

37. Steinem, C., A. Janshoff, F. Höhn, M. Sieber, and H.-J. Galla. 1997. Proton translocation across bacteriorhodopsin containing solid supported lipid bilayers. *Chem. Phys. Lipids.* 89:141–152.

38. Renthal, R., and C. H. Chan. 1984. Charge asymmetry of the purple membrane by uranyl quenching of dansyl fluorescence. *Biophys. J.* 55:581–583.

39. Khorana, H. G., G. E. Gerber, W. C. Herlihy, C. P. Gray, R. J. Anderegg, K. Nihei, and K. Biemann. 1979. Amino acid sequence of bacteriorhodopsin. *Proc. Natl. Acad. Sci. USA.* 76:5046–5050.

40. Le Blanc, O. H. 1971. Effect of uncouplers of oxidative phosphorylation on bilayer membranes: Carbonylcyanide-m-chlorophenylhydrazone. *J. Membr. Biol.* 4:227–251.

41. Müller, D. J., F. A. Schabert, G. Bueldt, and A. Engel. 1995. Imaging purple membranes in aqueous solutions at sub-nanometer resolution by atomic force microscopy. *Biophys. J.* 68:1681–1686.